Energy Fuels **2010,** *24,* 2634–2641 · DOI:10.1021/ef9009185
Published on Web 03/30/2010

energy&fuels
article

Fischer−Tropsch Synfuels from Biomass: Maximizing Carbon Efficiency and Hydrocarbon Yield

Dominik Unruh, Kyra Pabst, and Georg Schaub*

Engler-Bunte-Institut, Bereich Gas, Erdöl und Kohle, Karlsruher Institut für Technologie (KIT), Engler-Bunte-Ring 1, 76131 Karlsruhe, Germany

Received August 24, 2009. Revised Manuscript Received February 18, 2010

According to various published process studies, efficiencies of biomass-to-liquid conversion may be expected in the range of 30−50% for chemical energy and 25−45% for carbon recovered in hydrocarbon products. Strategies for improving carbon conversion efficiency include minimizing O_2 consumption in gasification and increasing synthesis selectivities and CO_2 conversion during synthesis with hydrogen added from external sources. CO_2 conversion during Fischer−Tropsch (FT) synthesis is possible with a CO/CO_2 shift-active catalyst, if sufficient H_2 is available. A combined experimental and modeling study has shown that equilibrium and kinetic limitations involved can be decreased by means of a membrane, which allows for *in situ* removal of H_2O from the catalyst bed. The results help to quantify the effects of H_2O permeability, permselectivities, and reaction conditions and help to indicate directions for further membrane development. This paper collects yield and efficiency estimates for FT synfuel production from biomass feedstocks. Limiting factors for the heating value output are discussed, and a conceptual/experimental study is presented that addresses *in situ* H_2O removal by a hydrophilic membrane, aiming at maximizing carbon efficiency.

Introduction

General Background. Conversion of biomass to liquid hydrocarbon fuels via Fischer−Tropsch (FT) synthesis is presently considered as attractive for biofuel production [biomass-to-liquid (BTL), "second-generation" biofuels]. In comparison to other biofuels, advantages include (i) flexible use of all kinds of biomass feedstocks (including waste materials) and, therefore, no competition with the production of food, (ii) relatively high yields per arable land (100−180 GJ ha^{-1} $year^{-1}$), and (iii) high fuel qualities to be used in present distribution infrastructures and high-efficiency engine technologies. As a disadvantage, overall process economics may be critical, given the high complexity of the chemical conversion process and the need for large-capacity plants for positive scale-up effects. As a first commercial application, a 15 000 tons/year BTL plant will shortly start operation in Freiberg, Germany.[1] In Europe, despite their expected high production cost, synthetic biofuels have played an important role in political discussions, besides first-generation ethanol and biodiesel fuels.

Liquid Synfuel Production from Solid Feedstocks via FT Synthesis. Traditional FT synthesis as practiced today on commercial scale uses H_2/CO syngas generated from coal or natural gas. In the case of biomass as raw material, analogous to coal, synthesis gas production occurs via oxygen/steam gasification or partial oxidation reactions (Figure 1).[2,3] The synthesis gas then has to be cleaned from impurities and adjusted to synthesis requirements. In low-temperature FT synthesis, long-chain waxy hydrocarbon molecules (C_{21+}) are produced with a characteristic distribution of individual hydrocarbon compounds, analogous to polymerization. Among different FT process alternatives, proper selection of the catalyst and reactor type may be significant for overall product yield and economics.[4,5] Upgrading of primary FT products most commonly includes hydroprocessing (cracking and isomerization) to produce a maximum yield of high-quality

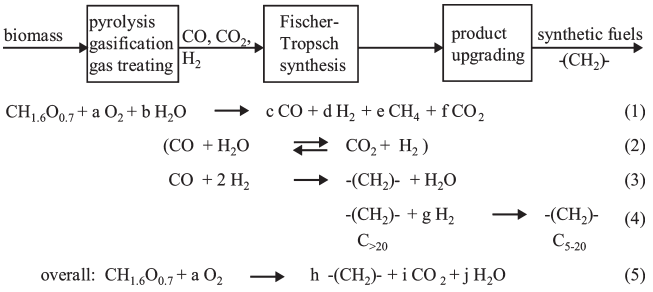

Figure 1. Flow scheme for the conversion of biomass feedstocks to liquid hydrocarbon fuels (BTL) and formal chemical reactions.

*To whom correspondence should be addressed. Telephone: +49-721-608-2572. Fax: +49-721-606172. E-mail: georg.schaub@kit.edu.

(1) Blades, T.; Rudloff, M.; Schulze, O. Sustainable SunFuel from CHOREN's Carbo V Process. Conference ISAF XV, San Diego, CA, 2005; www.choren.com/dl.php?file=San_Diego_-_Final.pdf (accessed on Nov 2009).

(2) Tijmensen, M.; Faaij, A.; Hamelinck, C.; van Hardeveld, M. *Biomass Bioenergy* **2002**, *23*, 129–152.

(3) Schaub, G.; Unruh, D.; Rohde, M. In *Biomasse-Vergasung—Der Königsweg für eine effiziente Strom- und Kraftstoff-Bereitstellung?* Landwirtschaftsverlag GmbH: Münster, Germany; 2004; Schriftenreihe Nachwachsende Rohstoffe 24, pp 351−362.

(4) Van Steen, E.; Claeys, M. *Process. Chem. Eng. Technol.* **2008**, *31*, 655–666.

(5) Guettel, R.; Kunz, U.; Turek, T. *Chem. Eng. Technol.* **2008**, *31*, 746–754.

(6) Dimmig, T.; Olschar, M. Sekundärenergieträger aus Biomasse—Eine systemanalytische Untersuchung. Final Report, Research Project BMVEL, 2003.

Table 1. Yield and Efficiency Values (Carbon or Heating Value Ratio of Liquid Hydrocarbon Products and Biomass Feedstock) from FT Synfuel Process Studies

		Tijmensen et al.[2]	Dimmig et al.[6]	Dena[7]	Leible et al.[8]
feed flow dry	tons/h	80[a]	100[a]	100[a]	18/900[b]
	GW	0.37[a]	0.5[a]	0.5[a]	0.1/5[a]
product flow $-(CH_2)-$[c]	tons/h	10−15	18	15−17[d]	119−139[d]
gasoline	tons/h			6−7	
diesel	tons/h			9−10	
η_{carbon}[e]	%	23−41	36	34	23−27
η_{H_s}[f]	%	32−51	45	42	29−34

[a] Basic definition. [b] Calculated with 18 (or 20) MJ/kg H_s (H_s = higher heating value). [c] Fuels C_{5-20}. [d] Calculated with 44 MJ/kg H_s. [e] m_C in C_{5-20}/m_C in biomass feed. [f] H_s of C_{5-20}/H_s of biomass feed.

Table 2. Overall Yields of Synthetic Hydrocarbon Products from Various Feedstocks in Comparison to Natural Hydrocarbons from Petroleum[a]

				η_{Hs} (%)
biomass[b]	100 $CH_{1.6}O_{0.7}$	⟶	23 – 41 $-(CH_2)-$	32 – 51
coal[c]	100 $CH_{0.6}O_{0.1}$	⟶	28 – 40 $-(CH_2)-$	35 – 50
natural gas[d]	100 CH_4	⟶	68 – 80 $-(CH_2)-$	53 – 63
petroleum[e]	100 $CH_{1.8}$	⟶	94 $-(CH_2)-$	94

[a] η_{H_s} = conversion efficiency based on the higher heating value (see Table 1). [b] From Tijmensen et al.[2] [c] From Hoogendorn.[9] [d] From Audus et al.[10] and Sie et al.[11] [e] Our own estimate for petroleum refining (as total).

Table 3. Stoichiometry of the Overall FT Biofuel Process for Expected Efficiency Values η_{H_s} (eqs 6 and 7) and Idealized Situations (eqs 8−10), without Specification of Individual Process Steps of Gasification, Synthesis, and Product Upgrading

expected real situations

$$100\ CH_{1.6}O_{0.7} + 45\ O_2 \xrightarrow{\eta_{Hs}\ 50\%} 40\ -(CH_2)- + 60\ CO_2 + 40\ H_2O \quad (6)$$

$$100\ CH_{1.6}O_{0.7} + 69\ O_2 \xrightarrow{\eta_{Hs}\ 30\%} 24\ -(CH_2)- + 76\ CO_2 + 56\ H_2O \quad (7)$$

idealized stoichiometric situations

$$100\ CH_{1.6}O_{0.7} \longrightarrow 70\ -(CH_2)- + 30\ CO_2 + 10\ H_2O \quad (8)$$

$$100\ CH_{1.6}O_{0.7} + 90\ CH_4 \longrightarrow 190\ -(CH_2)- + 70\ H_2O \quad (9)$$

$$100\ CH_{1.6}O_{0.7} + 90\ H_2 \longrightarrow 100\ -(CH_2)- + 70\ H_2O \quad (10)$$

fuels. Gasification of the solid feedstock with H_2O is an endothermic reaction. It requires high temperatures according to the reactivity of the solid, whereas FT synthesis, an exothermic reaction, is carried out at temperatures around 200−250 °C, if low-temperature FT synthesis conditions are applied, significantly lower than gasification. This leads to maximum yields of long-chain hydrocarbons that can be converted in a product upgrading step to the desired fuel product diesel.

Because there is no practical experience with large-scale BTL plants thus far, overall mass balance and achievable product yields have to be estimated on the basis of extrapolations from coal or gas as feedstock. Various studies have recently been published with estimated yield and efficiency values of the overall process based on flowsheet simulations. These studies indicate that efficiencies in terms of chemical energy and carbon recovered in the hydrocarbon product may be expected in the range of 30−50 and 25−45%, respectively (Table 1). Given the shortage of arable land and water in many countries, there is a need to achieve maximum fuel yields per unit of land. In addition to high biomass yields in agriculture and forestry, high conversion efficiencies in biomass processing are required. Similar to biomass feedstocks, overall yields of synfuel products from coal or natural gas are significantly lower than the fuel yields from petroleum refining (Table 2).

The present study is motivated by the most recent discussion in Europe about synthetic biofuels. Here, the aspect of achieving highest yields of liquid fuels per unit of biomass is ranked as highly significant, because heat and electricity can be more easily produced from other (renewable) resources.

Strategies for Carbon Efficiency Improvement

The overall conversion of biomass to synthetic hydrocarbons can be represented by stoichiometric equations (eq 5 in Figure 1). The overall stoichiometry includes gasification with oxygen and/or steam, CO shift, FT synthesis (leading to H_2O as the byproduct), and product upgrading. Equations 6 and 7 in Table 3 represent two cases with a recovery of chemical energy (as higher heating value, H_s) of 50 and 30%, respectively. The real case, as expected according to Table 1, will most likely be between these two cases. As a limiting case, eq 8 describes the conversion of biomass with no external oxygen required (for heat generation), i.e., an idealized situation, where the reaction would take place at ambient conditions. Energy efficiency in this case would be 87%, with a synfuel yield of 0.40 ton/ton of liquid hydrocarbon product C_{5-20} per dry and ash-free biomass, as compared to 0.23 and 0.14 ton/ton, respectively. Two additional idealized situations including the addition of hydrogen (in the form of CH_4 or H_2) are shown in eqs 9 and 10. Here, hydrocarbon yields are increased such that all carbon present in the feedstock biomass would be converted to hydrocarbons. This reflects a situation where the maximum use of biomass carbon is made for the production of liquid hydrocarbon synfuels.

The limited carbon or chemical energy efficiency of the overall process can be attributed to the following factors. (i) Overall stoichiometry: How much chemical energy can be

(7) Deutsche Energie-Agentur GmbH (Dena). Biomass to Liquid—BtL. Realisierungsstudie (Summary). Final Report, 2006.

(8) Leible, L.; Kälber, S.; Kappler, G.; Lange, S.; Nieke, E.; Proplesch, P.; et al. Kraftstoff, Strom und Wärme aus Stroh und Waldrestholz—Eine systemanalytische Untersuchung. Wissenschaftliche Berichte FZKA 7170. Forschungszentrum Karlsruhe GmbH, Karlsruhe, Germany, 2007.

(9) Hoogendorn, J. C. Gas from coal for synthesis of hydrocarbons. Presented at the 23rd Annual Meeting of the American Institute of Mining Engineers, 1974. Jüntgen, H.; Klein, J.; Knoblauch, K.; Schröter, H.-J.; Schulze, J. In *Chemistry of Coal Utilization*; Elliott, M. A., Ed.; John Wiley and Sons: New York, 1981; Supplementary Vol. 2, pp 2071−2158.

(10) Audus, H.; Choi, G.; Heath, A.; Tam, S. *Stud. Surf. Sci. Catal.* **2001**, *136*, 519–524.

(11) Sie, S. T.; Senden, M. M. G.; van Wechem, H. M. H. *Catal. Today* **1991**, *8*, 371–394.

Table 4. Composition of Dry Synthesis Gas from Biomass for Entrained Flow and Fluidized-Bed Gasification Processes[a]

gasification process	p	medium	$x_{i,\mathrm{dry}}$ (vol %) H_2	CO	CO_2	CH_4	x_{H_2}/x_{CO}	z_{H_2}[b]	z_{CO_2}[c]
entrained flow[d]	el	O_2	30	50	17	0.1	0.60	0.20	0.25
entrained flow[e]	atm/el	O_2	35.2	41.1	22.0	0.1	0.86	0.24	0.35
fluidized bed[f]	atm	H_2O	52.4	28.7	16.8	2.1	1.83	0.48	0.37
fluidized bed[g]	el	O_2/H_2O	31.0	38.6	27.2	3.1	0.80	0.20	0.41

[a] atm/el = near ambient/elevated pressure. [b] $z_{H_2} = x_{H_2}/(2x_{CO} + 3x_{CO_2})$. [c] $z_{CO_2} = x_{CO_2}/(x_{CO} + x_{CO_2})$. [d] From Henrich and Dinjus.[12] [e] From Althapp.[13] [f] From Hofbauer et al.[14] [g] From Lemasle.[15]

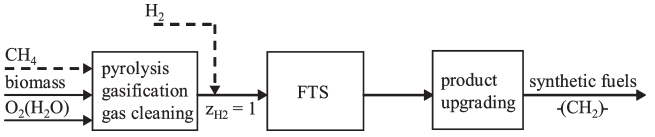

Figure 2. Strategies for carbon efficiency improvement in the FT biofuel process via the addition of (i) methane to gasification or (ii) hydrogen to FT synthesis, z_{H_2} (see Table 4).

stored according to the overall stoichiometry in the desired fuel product hydrocarbon; i.e., what is the heat of the overall reaction (where exothermicity means a loss in chemical energy)? (ii) Different temperature levels: How much heat is required for the endothermic gasification step, where the exothermic synthesis reaction, because of the low-temperature level, cannot contribute significantly? (iii) Energy requirements for continuous operation: Which are internal energy requirements of the process (e.g., high-pressure application, transport of solids and fluids, or size reduction of solids)? (iv) Product selectivity: Which fraction of the reactants is converted to the desired products (e.g., to C_{5-20} hydrocarbons during FT synthesis and hydrocracking)?

As a result of biomass gasification, Table 4 gives representative values for the composition of dry synthesis gas for various gasification conditions (type of gasification process, pressure, and gasifying medium). High-temperature (entrained flow) processes exhibit lower methane and hydrogen contents (as CH_4 and H_2), reflecting a higher reaction temperature and higher oxygen consumption.

To improve the carbon conversion efficiency of the BTL process, the following strategies can be applied (Figure 2): (1) minimize O_2 consumption in gasification and exothermicity of the overall reaction, (2) improve hydrocarbon selectivity during synthesis and hydrocracking, and (3) add hydrogen (as CH_4 to gasification or as H_2 to FT synthesis) and allow for CO_2 hydrogenation.

Strategies 1 and 2 are being followed in the development of improved gasification processes or catalysts (e.g., for modifying Anderson–Schulz–Flory (ASF) product selectivities in FT synthesis). For strategy 3, conceptual reflections and a reactor concept for integrated CO_2 hydrogenation in FT synthesis will be presented in the following. A novel membrane reactor, allowing for *in situ* H_2O removal, should help to increase CO_2 conversion during FT synthesis with a Fe-based catalyst.

Minimization of O_2 Consumption in Gasification

For gasification of solid carbonaceous feedstocks (biomass and coal), different processes are available, characterized by the method of contacting the solid and gaseous reactants: moving bed, fluidized bed, and entrained flow. According to particle residence time and particle size, temperatures must be significantly different for each reactor concept to ensure appropriate chemical reaction rates. Because the heat for the endothermic reactions and heating up the reactants is supplied by partial combustion of the feedstock with oxygen, higher temperature requires increased oxygen consumption. An increased O_2 consumption, however, leads to lower yields of synthesis gas CO/H_2 and, thus, synthetic hydrocarbons after FT synthesis (right panel of Figure 3). For synthesis gas production from biomass, entrained flow gasification is often preferred, because a high temperature applied leads to a tar-free gas as a result of complete tar conversion in gas-phase reactions and a low methane yield. In the case of coal as feedstock, the correlation between the O_2 consumption and gasification temperature/tar content was developed on the basis of a wide variety of experimental data[16] (left panel of Figure 3, as trends). Biomass in general is more reactive than coal and may allow for a lower gasification temperature and lower O_2 consumption, e.g., in fluidized-bed gasification. Hydrocarbon yield as affected by O_2 consumption is calculated on a stoichiometric basis, according to the formal reactions in Table 3.

Minimization of heat requirements in gasification will accordingly lead to maximum synthesis gas yields. Strategies include minimization of the temperature and internal use of process heat (e.g., using high exit temperatures for endothermic gasification reactions with H_2O or CO_2, "chemical quench").

CH_4 Feed to Gasification

The effect of cofeeding CH_4 to gasification of biomass can be estimated by an idealized stoichiometric approach. The resulting hydrocarbon yields are shown in Figure 4 as a carbon fraction of the biomass feed, for three different values of oxygen consumption (see the definition in Figure 3). For the assumed biomass stoichiometry $CH_{1.6}O_{0.7}$, methane amounts added to 10 and 50 mol % C correspond to specific volumes $V_{CH_4}/m_{CH_{1.6}O_{0.7}}$ in m^3/ton of biomass dry and ash free (daf) of 90.3 and 451.6, respectively.

Conversion of CH_4 to synthesis gas should occur at the conditions of high-temperature gasification (see examples in Table 4). This is an advantage of entrained flow processes whenever synthesis gas is the desired product (in contrast to fuel gas). CH_4 reacts in a combination of pyrolysis, partial oxidation, and steam reforming reactions, similar to the

(12) Henrich, E.; Dinjus, E. In *Biomasse-Vergasung—Der Königsweg für eine effiziente Strom- und Kraftstoff-Bereitstellung?*; Landwirtschaftsverlag GmbH: Münster, Germany, 2004; Schriftenreihe Nachwachsende Rohstoffe 24, pp 298–337.

(13) Althapp, A. Synthetic transportation fuels from biomass via Fischer–Tropsch synthesis—Priciples and perspectives. Conference "Regenerative Kraftstoffe", Stuttgart, Germany, 2003; pp 218–227.

(14) Hofbauer, H.; Rauch, R.; Foscolo, P.; Matera, D. Hydrogen-rich gas from biomass steam gasification. Proceedings of the 1st World Conference on Biomass for Energy and Industry, Sevilla, Spain, 2001; pp 1999–2001.

(15) Lemasle, J. In *Thermochemical Processing of Biomass*; Bridgewater, H. V., Ed.; Butterworths: London, U.K., 1984; pp 151–157.

(16) Schaub, G.; Reimert, R. Gas. In *Ullmann's Encyclopedia of Industrial Chemistry*, 6th ed.; Wiley-VCH: Weinheim, Germany, 2003; Vol. 15, pp 357–380.

(17) Riedel, T.; Schaub, G.; Jun, K.-W.; Lee, K.-W. *Ind. Eng. Chem. Res.* **2001**, *40*, 1355–1363.

(18) Claeys, M.; van Steen, E. In *Studies in Surface Science and Catalysis 152: Fischer–Tropsch Technology*; Steynberg, A., Dry, M., Eds.; Elsevier: Amsterdam, The Netherlands, 2004; pp 601–680.

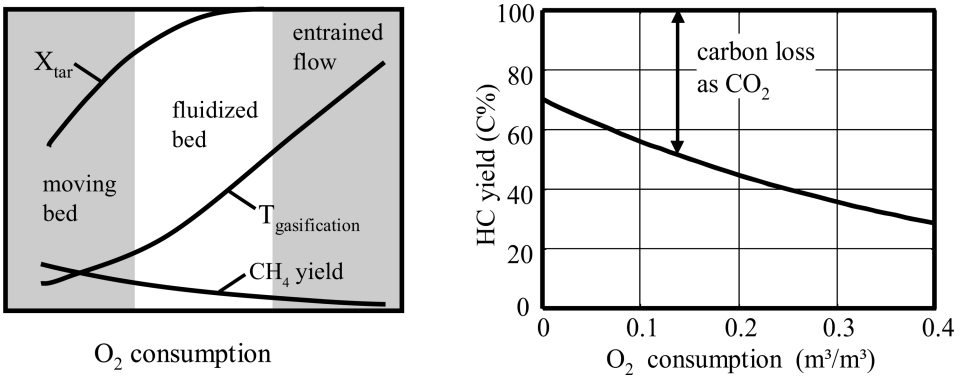

Figure 3. Oxygen consumption $V_{n,O_2}/V_{n,(CO+H_2)}$, methane yield, and tar conversion correlated with the gasification temperature (schematic, left) and the calculated effect on the overall FT synfuel yield (in C %, on the basis of stoichiometry, according to eqs 6−8 in Table 3, right).[3]

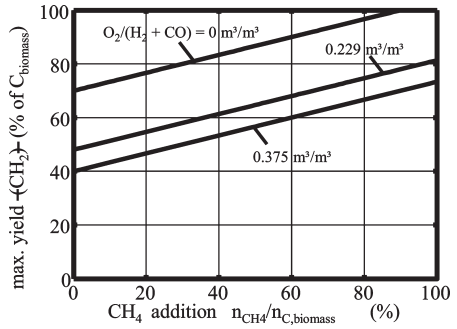

Figure 4. Effect of the CH_4 addition to syngas production on the overall hydrocarbon product yield (estimate based on simplified stoichiometry and biomass carbon only). Parameter = O_2 consumption in gasification (see Figure 3).

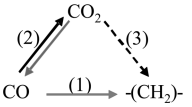

		$\Delta_R H$	
$CO + 2\,H_2 \longrightarrow$	$-(CH_2)- + H_2O$	$<< 0$	(1)
$CO_2 + H_2 \rightleftharpoons$	$CO + H_2O$	> 0	(2)
$CO_2 + 3\,H_2 \longrightarrow$	$-(CH_2)- + 2\,H_2O$	$<< 0$	(3)

Figure 5. Reaction network of CO_2 hydrogenation for K-promoted Fe catalyst: (1) FT reaction, (2) CO_2/CO shift reaction, and (3) direct CO_2 hydrogenation.[17]

situation in autothermal reforming processes.[19,20] CH_4 conversion is limited by chemical equilibrium (e.g., down to 0.3% CH_4 content at 1000 °C, 20 bar, and molar ratio of steam/methane at 3.3)[20] and reaction kinetics. The prediction of steam and oxygen requirements is difficult, because of the complex reactions occurring. In Figure 4, O_2 consumption referred to the synthesis gas yield from biomass is therefore indicated as the parameter. Accordingly, higher oxygen consumption because of CH_4 addition will lower the increase of the hydrocarbon yield from biomass.

Hydrogen Addition and CO_2 Conversion

Limiting Factors. For stoichiometry reasons, the H_2 content in the synthesis gas has to be increased to a z_{H_2} value of a minimum of 1 (Table 4). In this case, hydrogenation of CO_2 first to CO and then to hydrocarbons can take place according to the reaction network in Figure 5.[17]

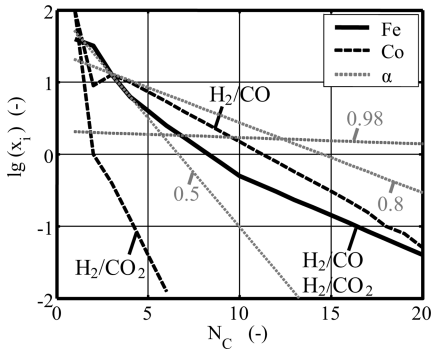

Figure 6. Typical hydrocarbon product distributions of Fe- and Co-based catalysts (as mole fraction x_i versus carbon number N_C). Examples measured in lab scale (black lines): $Fe/Al_2O_3/Cu/K$ and $Co/MnO/SiO_2/Pt$ catalyst, H_2/CO and H_2/CO_2 synthesis gas, fixed-bed reactor (2 g of catalyst), T = 190 °C (Co)/250 °C (Fe), p = 1 MPa, $(p_{H_2}/p_{CO_x})_{in}$ = 2 (Co)/2.3 (Fe), and τ_{mod} = 4000 kg s m^{-3}. Gray dotted lines = calculated with different α values.

Because direct hydrogenation to hydrocarbons (eq 3 in Figure 5) is not significant, the indirect hydrogenation via CO as the intermediate is dominating. Therefore, the overall reaction of CO_2 to hydrocarbons is controlled by chemical equilibrium criteria (CO_2/CO shift) as well as kinetic criteria (catalyst activity and residence time).[17] Because the CO_2/CO shift is not favored at the low temperatures of FT synthesis (200−250 °C), the chemical equilibrium limitation can be avoided by removing CO (which is occurring because of FT reactions) or removing H_2O. In contrast, the H_2O formed as the byproduct of FT synthesis favors the formation of CO_2. The reaction network in Figure 5 leads to the same hydrocarbon product distributions for CO_2 as for CO as the reactant. This is valid for the Fe catalyst, as can be seen in Figure 6. For a Co catalyst, there is only limited chain propagation with H_2/CO_2 as the feed gas, because Co has almost no CO_2/CO shift activity. Feeding CO, the amount of long HC chains is larger for the Co catalyst than for the Fe catalyst.

The carbon number distribution of the product is characterized by a linear correlation of the molar fraction of species i [as $\log(x_i)$] and carbon number N_C (ASF distribution), with the parameter being the logarithmized chain propagation value α as the slope (in Figure 6). Generally, the chain propagation decreases with an increasing temperature and molar ratio of H_2/CO. This is especially valid for the Co

(19) Aasberg-Petersen, K.; Christensen, T. S.; Dybkjær, I.; Sehested, J.; Østberg, M.; Coertzen, R. M.; et al. In *Studies in Surface Science and Catalysis 152: Fischer−Tropsch Technology*; Steynberg, A., Dry, M., Eds.; Elsevier: Amsterdam, The Netherlands, 2004; pp 258−405.

(20) (a) Marschner, F.; Renner, H.-J.; Boll, W. In *Ullmann's Encyclopedia of Industrial Chemistry*, 6th ed.; Wiley-VCH: Weinheim, Germany, 2003; Vol. 15, pp 325−357. (b) Supp, E.; Brejc, M.; Liebner, W. In *Ullmann's Encyclopedia of Industrial Chemistry*, 6th ed.; Wiley-VCH: Weinheim, Germany, 2003; Vol. 15, pp 325−357.

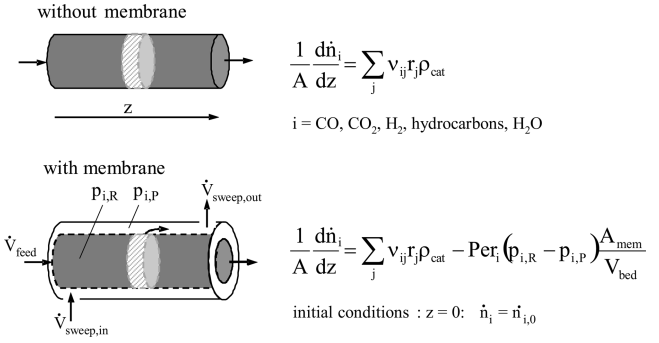

Figure 7. Schematic effect of H_2O removal with a hydrophilic membrane and basic equations of the fixed-bed reactor model (catalytic fixed bed, lab scale, steady state, plug flow, one-dimensional, pseudo-homogeneous, and isothermal).

Table 5. Permeance and Permselectivity Values Used in the Conceptual Studies (on the Basis of Kölsch et al.)[24]

Per H_2O	=	10^{-8},	10^{-7}	mol Pa^{-1} s^{-1} m^{-2}
S_{H_2O/H_2}	=	0.5,	∞ (ideal)	
$S_{H_2O/CO}$	=	12.5,	∞ (ideal)	
S_{H_2O/CO_2}	=	5,	∞ (ideal)	

catalyst because it normally has no CO_2/CO shift activity and cannot compensate for the disadvantageous H_2/CO ratio. In contrast, a higher partial pressure of CO or H_2O and also a higher total pressure leads to increased chain propagation.[18]

***In Situ* H_2O Removal from the FT Reactor with Membrane.** *Concept and Simulated Case Studies*. In a catalytic synthesis reactor, a Fe-based FT catalyst allows for both CO_2/CO shift and FT synthesis reactions to occur. A mathematical modeling study for a fixed-bed reactor with a H_2O-permeable membrane as the reactor wall helps to simulate a lab-scale experiment on the basis of kinetic information from the literature (Figure 7).[21]

The model, which serves as a tool to design experiments and analyze experimental results, includes parameter values for membrane transport (Table 5) and kinetic rate equations of the FT and CO_2/CO shift reactions.[22] The lab-scale reactor used in the later experiments can be modeled as a steady-state, one-dimensional, isothermal plug-flow reactor. Transport through the membrane, which, in the present case, consists of tetraethyl-orthosilicate (TEOS) on an ultrafiltration support (γ-Al_2O_3 or α-Al_2O_3),[23] is described by a solution-diffusion mechanism. Transmembrane molar flow is assumed to be proportional to the partial pressure difference across the membrane and the permeance Per_i. The permselectivity S_{ij} is given as the ratio of two permeances Per_i/Per_j.

Calculated profiles of conversion and hydrocarbon yields are shown in Figure 8 for the two syngas cases H_2/CO (left) and H_2/CO_2 (right). For H_2/CO_2 syngas, the reaction network with CO as the intermediate product (Table 5) is reflected by the maximum in Y_{CO}. Hydrogenation of CO is much faster than hydrogenation of CO_2, leading to higher conversion and higher hydrocarbon yields. Integration of an ideal permselective membrane, for H_2/CO_2 syngas, has a positive effect on the CO_2 conversion and hydrocarbon yield (dotted versus full curves).

For mixed CO/CO_2 syngas, as in real gasification processes shown in Table 4, calculated effects of a H_2O-selective membrane are shown in Figure 9. The x axis covers the range between the extremes of syngas H_2/CO and syngas H_2/CO_2 (equivalent to $z_{CO_2} = 0$ or 1, respectively).

Negative values of X_i mean the formation of component i. For the Fe catalyst considered, a strong effect of H_2O permeance (i.e., H_2O removal) on CO_2 conversion and thus total hydrocarbon yield (Y_{HC}) can be seen. This result motivated the effort for experimental demonstration of an integrated membrane for *in situ* removal of H_2O.

Experimental Demonstration of in Situ H_2O Removal with Integrated Membrane. On the basis of the simulated case studies, experiments were carried out in a lab-scale fixed-bed membrane reactor at conditions where the strongest effects of H_2O removal can be expected.[21,25] The membrane (L = 300 mm, d = 10 mm, and s = 1.5 mm) is fixed with two high-temperature gaskets (Figure 10). Because the functional layer is on the inside of the membrane, the catalyst is filled into the membrane tube. The feed gas enters the reactor from the top, and the sweep gas flows in cocurrent mode through the angular channel between the membrane and reactor shell. The flow rates and pressures on the feed and sweep sides can be adjusted independently. The long-chain hydrocarbons in the retentate flow are collected in a hot wax trap (175 °C and 1 MPa) before the retentate and permeate flow are led to the online gas chromatography (GC) analysis. The experiments were carried out with 2 g of K-promoted, Fe-based catalyst (d_P = 100−160 μm; diluted with 8 g of quartz sand, d_P = 160−200 μm) at a fixed feed gas flow rate and a feed gas composition of H_2/CO_2 (3:1). The membrane tubes used are coated with three layers of TEOS (provided by the former Institut für Angewandte Chemie Adlershof).

Because of the low hydrothermal stability of the functional layer, the catalyst is calcined, reduced with H_2, and activated with H_2/CO (2:1) in a separate fixed-bed reactor. While the catalyst was filled into the membrane tube, re-oxidation or deactivation was not observed as a result of the presence of wax on the catalyst, even under short exposure to air. The following conditions were varied: (i) sweep gas composition [Ar, H_2, or H_2/CO_2 (3:1)], (ii) sweep flow ratio (between 1.7 and 6.7), and (iii) temperature (225 and 250 °C). Pressure on the sweep side is kept at 100 mbar above the pressure on the feed side (1 MPa).

With H_2/CO_2 as the sweep gas, simulating a selective membrane for H_2O, conversion of CO_2, and total hydrocarbon yield are increased by H_2O removal. The left panel of Figure 11 shows the experimental data as well as calculated profiles along the reactor length. Variations in the sweep ratio between 0 and 6.7 with effects on conversion and yields are shown in the right panel of Figure 11.

The model calculations are based on kinetic parameter values and rate equations for the FT catalyst used, measured in separate experiments (Table 6). Permeance values were treated as adjustable parameters, leading to values close to

(21) Unruh, D. Fischer−Tropsch Synthese mit Synthesegasen aus Biomasse—Verbesserung der Kohlenstoffnutzung durch Anwendung eines Membranreaktors. Ph.D. Dissertation, Universität Karlsruhe (TH). Shaker Verlag, Aachen, Germany, 2006.

(22) Riedel, T. Reaktionen von CO_2 bei der Fischer−Tropsch Synthese—Kinetik und Selektivität. Ph.D. Dissertation, Universität Karlsruhe (TH). Shaker Verlag, Aachen, Germany, 2003.

(23) Noack, M.; Kölsch, P.; Schäfer, P.; Toussaint, P.; Caro, J. *Chem. Eng. Technol.* **2002**, *25*, 221–230.

(24) Kölsch, P.; Sziladi, M.; Noack, M.; Caro, J.; Kotsis, L.; Kotsis, I.; Sieber, I. *Chem. Ing. Tech.* **2000**, *72*, 1167–1173.

(25) Rohde, M.; Unruh, D.; Schaub, G. *Ind. Eng. Chem. Res.* **2005**, *44*, 9653–9658.

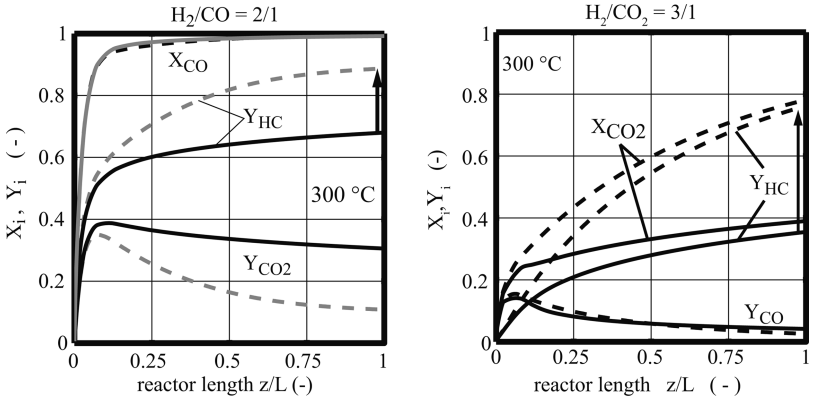

Figure 8. Calculated profiles of conversion X and yields Y for H_2/CO (left) and H_2/CO_2 synthesis gas (right). Effect of H_2O removal via ideal membrane (dotted versus full curves): $T = 300$ °C, $p = 1$ MPa, $\tau_{mod} = 2000$ kg s m^{-3}, $A_{mem}/m_{cat} = 3$ m^2 kg^{-1}, sweep ratio > 3, and $Per_{H_2O} = 10^{-7}$ mol Pa^{-1} s^{-1} m^{-2}.

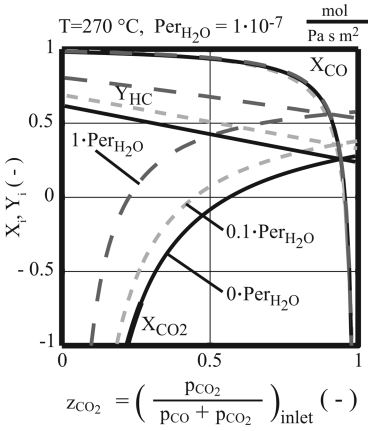

Figure 9. Conversion X of CO, CO_2, and HC yield versus CO_2 content in synthesis gas calculated for fixed-bed reactor conditions with the kinetic model. Effect of the ideal permselective membrane: $T = 270$ °C, $p = 1$ MPa, $\tau_{mod} = 2000$ kg s m^{-3}, $A_{mem}/m_{cat} = 3$ m^2 kg^{-1}, sweep ratio = 3.3, and $Per_{H_2O} = 10^{-7}$ mol Pa^{-1} s^{-1} m^{-2}.

those in Table 5 (Per_i $H_2O/H_2/CO_2/CO$ = 0.76/2.0/0.02/0.08 × 10^{-7} mol Pa^{-1} s^{-1} m^{-2}). The situation with zero sweep gas ratio is equivalent to a fixed bed without a membrane. Increasing the sweep ratio means increasing the rate of H_2O removal, thus increasing the positive effect on CO_2 hydrogenation rates.

Using the experimental information on chemical reaction and transmembrane transport rates, simulation studies will quantify the positive effects of H_2O removal on CO_2 conversion and hydrocarbon yields. A critical aspect is the low H_2O permeance through the membrane, leading to high specific membrane areas (A_{mem}/V_{cat}), which, for practical applications, would have to be lowered significantly. The present results and further experiments with other types of membranes and reactor engineering studies in our laboratories[26,27] will lead to a quantitative assessment of *in situ* H_2O removal during FT synthesis and give directions for future development of membranes.[28]

Economic Aspects

Feasibility studies for actual BTL plant designs in Germany consider plant capacities of typically 120 kilotons year^{-1} of liquid hydrocarbon fuels.[7] The investment figures for various technology alternatives are reported in the range of 525−650 Mio euro (estimates ±30%),[7] including mechanical pretreatment, air separation, entrained flow gasification, synthesis gas cleaning, FT synthesis, and product upgrading. The resulting fuel production cost is about 24 euro GJ^{-1} (higher heating value), if biomass costs of 4 euro GJ^{-1} are assumed.[7,29] Maximizing carbon efficiency according to the strategies discussed in the present paper would affect the process economics as outlined in the following.

Applying fluidized-bed gasification with lower O_2 consumption helps to decrease air separation requirements and related cost (or even avoid it if steam is used as the fluidizing gas).[14] However, higher methane and tar yields may lead to a lower liquid hydrocarbon yield, which increases specific production cost. Co-production of liquid fuels and methane as substitute natural gas (and potentially electricity and heat) would lessen this effect.

CH_4 feed to gasification would possibly lead to a higher gasification temperature and, thus, a higher oxygen requirement, resulting in a higher air separation cost.

Application of H_2O-permeable membranes for *in situ* removal in FT reactors, for which the principle was demonstrated in this study, will be difficult and costly because of (i) large membrane areas required as a result of low permeabilities, (ii) loss of syngas components as a result of low permselectivities, and (iii) competing requirements of membrane and heat-transfer areas, resulting in complex reactor designs. Significant improvements in developing membrane materials would be needed.

Summary and Conclusion

Chemical conversion of biomass via FT synthesis involves endothermic reactions at high temperature and exothermic reactions at lower temperatures, leading to a significant loss in

(26) Rohde, M.; Schaub, G.; Vente, J. F.; Van Veen, H. M. Fischer−Tropsch synthesis with in situ H_2O removal by a new hydrophilic membrane—An experimental and modelling study. Conference "Synthesis Gas Chemistry", Dresden, Germany, 2006; DGMK-Report 2006-4, pp 215−222.

(27) Rohde, M.; Schaub, G.; Khajari, S.; Jansen, J. C.; Kapteijn, F. *Microporous Mesoporous Mater.* **2008**, *115*, 123–136.

(28) Rohde, M. In situ H_2O removal via hydrophilic membranes during Fischer−Tropsch and other fuel-related synthesis reactions. Ph.D. Dissertation, Universität Karlsruhe (TH), Karlsruhe, Germany, 2010.

(29) Renewable Fuels for Advanced Powertrains (ReNew). EU Research Project, Executive Summary, 2008; www.renew-fuel.com/fs_documents.php (accessed on Feb 2010).

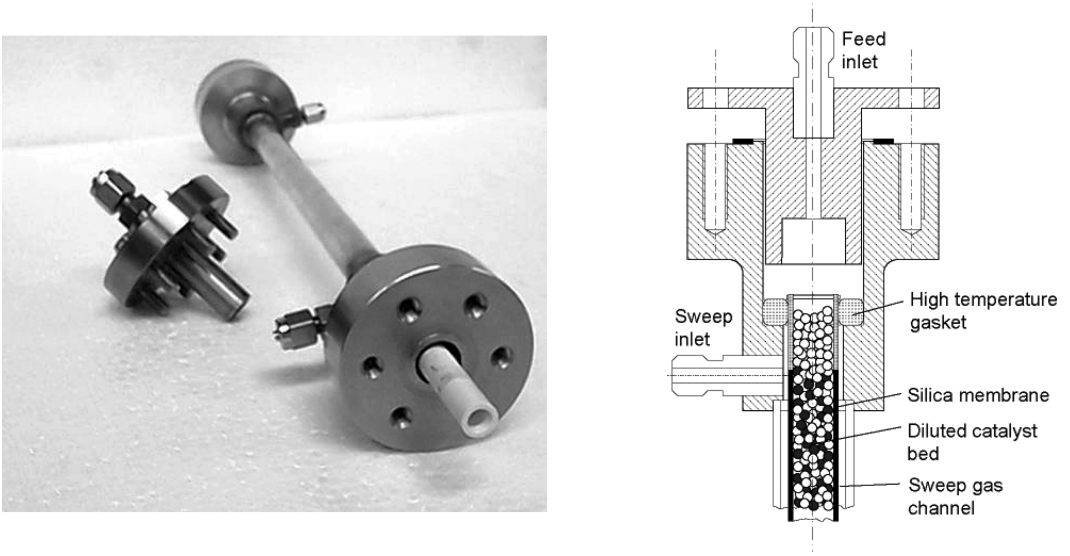

Figure 10. Lab-scale fixed-bed reactor for FT synthesis experiments with integrated membrane, 2 g of catalyst, and $A_{mem}/m_{cat} = 3\ m^2\ kg^{-1}$.

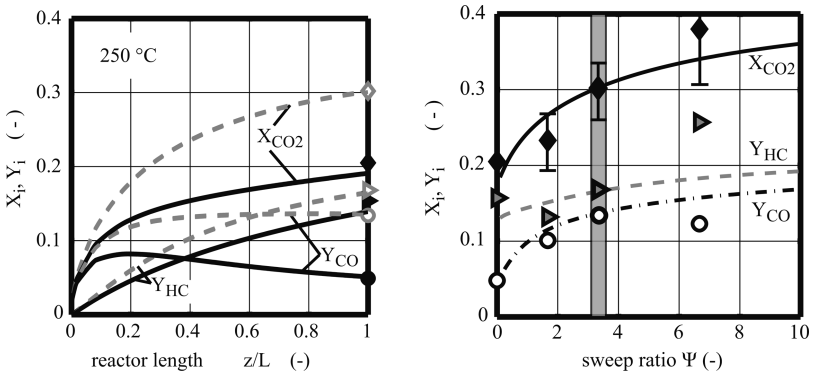

Figure 11. Measured effects on conversion and yield of (a) membrane integration (full/empty symbols = without/with membrane) (left) and (b) sweep ratio (right) curves. Model calculation with permeances as adjustable parameters: syngas and sweep gas, $H_2/CO_2 = 3$, $T = 250$ °C, $p = 1$ MPa, $m_{cat} = 2$ g, and sweep flow = 0.50, 100, and 200 $cm^3\ min^{-1}$.

Table 6. Rate Equations Used for the FT Reaction and CO_2 Shift Reaction and Kinetic Parameter Values[a]

$$r'_{FT} = k'_{FT}\frac{p_{CO}p_{H_2}}{p_{CO} + a_{FT,H_2O}p_{H_2O} + b_{FT,CO_2}p_{CO_2}}$$

$$r'_{CO_2-SH} = k'_{CO_2-SH}\frac{p_{CO_2}p_{H_2} - p_{CO}p_{H_2O}K_{P,CO-SH}}{p_{CO} + a_{SH,H_2O}p_{H_2O} + b_{SH,CO_2}p_{CO_2}}$$

$$\log K_{P,CO-SH} = (2073/T - 2.029)$$

			FT	CO_2−SH
k'_f ($\times 10^9$)	mol s^{-1} kg^{-1} Pa^{-1}	225 °C	1.55	1.73
		250 °C	2.50	4.69
a_{j,H_2O}	Pa^{-1}		1.12	15.01
b_{j,CO_2}' ($\times 10^5$)	Pa^{-1}		2.32	0.79

[a] Nonlinear regression of the experimental data: $Fe/Al_2O_3/Cu/K$ (100:13:10:5 wt), $p = 1$ MPa, $(p_{H_2}/p_{CO_2})_{F,in} = 3{:}1$, and $\tau_{mod} = 1000$–4000 kg s m^{-3}.

chemical energy and limited carbon recovery in the product. Besides the minimization of the O_2 consumption in gasification and the improvement of the product selectivity during synthesis, the addition of hydrogen is a potential strategy for improving carbon conversion efficiency. The hydrogen added (in the form of CH_4 or H_2) can help increase the conversion of CO and CO_2 during synthesis. As for CO_2, there is a chemical equilibrium limitation (according to the CO_2/CO shift) and also a kinetic reaction rate limitation.

Increased CO_2 conversion can be achieved if H_2O is removed *in situ* by a selective membrane, thus decreasing limitations for CO_2 hydrogenation. The combined theoretical and experimental study shows (i) measurable effects of membrane integration in a lab-scale fixed-bed FT reactor, with positive effects of H_2O permeance, permselectivities, sweep ratio, etc., (ii) permselectivities of a ceramic example membrane being too low, with compensation using syngas as sweep gas, and (iii) directions for membrane development, i.e., benchmarks for membrane permeances and permselectivities. Accordingly, new types of membranes are being developed.[26,27]

Application of membranes as a strategy toward maximized carbon efficiency will affect plant economics in a complex way. Most critical are the large membrane areas required, because of low membrane permeabilities, which will compete with heat-transfer areas inside the reactor.

A quantitative assessment of the concept of *in situ* H_2O removal during FT synthesis and the potential beneficial

effects on reactor performance will result from an ongoing study.[28] Here, the potentials are being addressed with *in situ* H_2O removal via alternative methods (selective permeation through membranes, adsorption, and chemical conversion) and also after an external CO_2 (reverse) shift reactor combined with a FT reactor with a cobalt catalyst. Results regarding reactor analysis and practical process implications will be presented in a subsequent publication.

Acknowledgment. The authors gratefully acknowledge financial support from the German government (BMBF and ReFuelNet) and helpful discussions with Martin Rohde and Prof. Hans Schulz.

Nomenclature

A = area (m^2)
d = diameter (m)
H_s = higher heating value (MJ kg^{-1})
L = length (m)
m_{cat} = mass of catalyst (kg)
$\dot{n}_i$ = molar flow of component i (mol s^{-1})
N_C = number of carbon atoms
p = pressure (Pa)
p_i = partial pressure of component i (Pa)
Per_i = permeance of component i (mol Pa^{-1} s^{-1} m^{-2})
r_j = reaction rate of reaction j (mol kg^{-1} s^{-1})
s = thickness (m)
S_{ij} = permselectivity as Per_i/Per_j
t = time (s)
T = temperature (°C)
V_{bed} = volume of the catalyst bed (m^3)
x_i = mole fraction of component i
$x_{i,dry}$ = volume fraction of component i in dry gas
X_i = conversion of component i (mol of component i converted/mol of component i fed)
Y_i = yield of component i (mol of component i produced/mol of component j fed)
z = reactor axial length coordinate (m)
z_{H_2} = H_2 fraction for conversion of CO/CO_2 containing syngas
z_{CO_2} = CO_2 fraction of CO/CO_2 containing syngas

Greek Letters

α = chain growth probability as the ratio of rates of chain growth and sum of chain growth and desorption
η_{carbon} = carbon efficiency based on carbon mass
η_{H_s} = energy efficiency based on higher heating value
ν_{ij} = stochiometric coefficient of component i in reaction j
ρ = density (kg m^{-3})
τ_{mod} = modified residence time based on the catalyst mass as m_{cat}/inlet volume flow (kg s m^{-3})
Ψ = sweep ratio as the inlet syngas volume flow/inlet sweep gas volume flow